Inorganic Chemistry

Article

pubs.acs.org/IC

Synthesis and Characterization of the New Strontium Borogermanate $Sr_{3-x/2}B_{2-x}Ge_{4+x}O_{14}$ (x = 0.32)

Benedikt Petermüller, Lucas L. Petschnig, Klaus Wurst, Gunter Heymann, and Hubert Huppertz*

Institut für Allgemeine, Anorganische und Theoretische Chemie, Leopold-Franzens-Universität Innsbruck, Innrain 80-82, A-6020 Innsbruck, Austria

Supporting Information

ABSTRACT: The strontium borogermanate $Sr_{3-x/2}B_{2-x}Ge_{4+x}O_{14}$ (x = 0.32) was synthesized by high-temperature solid-state reaction of SrO, GeO_2, and H_3BO_3 in a NaF/KF flux system using platinum crucibles. The structure determination revealed that $Sr_{3-x/2}B_{2-x}Ge_{4+x}O_{14}$ (x = 0.32) crystallizes in the trigonal space group $P321$ (No. 150) with the parameters a = 800.7(2) and c = 488.8(2) pm, with $R1$ = 0.0281, $wR2$ = 0.0671 (all data), and Z = 1. The crystal structure of $Sr_{3-x/2}B_{2-x}Ge_{4+x}O_{14}$ (x = 0.32) consists of distorted SrO_8 cubes, GeO_6 octahedra, GeO_4 tetrahedra, and BO_4 tetrahedra. In addition to the structural investigations, Raman and IR spectroscopic investigations were carried out.

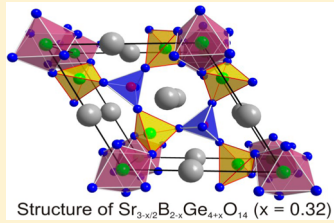

INTRODUCTION

Over the last couple of years, the class of metal borogermanates gained noticeable interest in the scientific community. This is in particular due to their interesting physical properties such as ferro-, pyro-, or piezoelectricity and nonlinear optical (NLO) properties, for example, in applications where these compounds could be used as second-harmonic-generation (SHG) materials.[1−5] SHG materials are mainly used as frequency doublers within various solid-state laser applications and are therefore very interesting for several industrial branches. Examples in the chemistry of borates are BBO (β-BaB_2O_4), LiB_3O_5, KBBF ($KBe_2BO_3F_2$), or BIBO (α-BiB_3O_6).[5−7] This SHG effect is generated by the arrangement of BO_3 and BO_4 groups,[8] asymmetrically coordinated transition metals (Ti^{4+}, Nb^{5+}, W^{6+}), or stereoactive cations with lone pairs (e.g., Se^{4+}, Te^{4+}, Sb^{3+}).[5,9−11] A couple of recently discovered alkali borogermanates such as $K_2GeB_4O_9{\cdot}2H_2O$, $Rb_4Ge_3B_6O_{17}$, CsB_3GeO_7, $AGeB_3O_7$ (A = Rb, Cs), or $A_2GeB_4O_9$ (A = Rb, Cs) also show NLO properties and distinct SHG effects.[1,3,12−14] Through the combination of different Ge−O units, for example, GeO_4 tetrahedra, trigonal GeO_5 bipyramids, or GeO_6 octahedra, borogermanates show a great diversity of structures. Most of these borogermanates possess a high thermal stability and a transparency within a wide range of frequencies.[5] Interestingly, only a few alkaline-earth borogermanates, namely, $Ba_3Ge_2B_6O_{14}$,[4] $Ba_3[Ge_2B_7O_{16}(OH)_2](OH)(H_2O)$,[4] and $Ca_{10}Ge_{16}B_6O_{51}$[2] are known. Just very recently, the first strontium borogermanates $SrGe_2B_2O_8$ and $Sr_3Ge_2B_6O_{16}$ were discovered. Obviously, Mao et al. became aware of the fact that no strontium borogermanate existed, and they were successful in synthesizing the above-mentioned two new representatives.[1]

In this work, we report the synthesis and structural characterization of a new strontium borogermanate with the composition $Sr_{3-x/2}B_{2-x}Ge_{4+x}O_{14}$ (x = 0.32) including its characterization via IR spectroscopy, Raman spectroscopy, and energy-dispersive X-ray (EDX) spectroscopy. In contrast to the above-mentioned two centrosymmetric borogermanates $SrGe_2B_2O_8$ (space group: $Pnma$) and $Sr_3Ge_2B_6O_{16}$ (space group: $P\bar{1}$) the here-described phase $Sr_{3-x/2}B_{2-x}Ge_{4+x}O_{14}$ (x = 0.32) crystallizes in the noncentrosymmetric space group $P321$. Taking into account that $Sr_{3-x/2}B_{2-x}Ge_{4+x}O_{14}$ (x = 0.32) is isotypic to $Ca_3Ga_2Ge_4O_{14}$[15,16] and $Sr_3Ga_2Ge_4O_{14}$,[17] this compound represents a new member of the family of langasites ($La_3Ga_5SiO_{14}$) possessing the general composition $A_3XY_3Z_2O_{14}$.[18] This class of compounds is highly interesting concerning their piezoelectric properties because nearly all 140 known members crystallize in the trigonal noncentrosymmetric space group $P321$.[19,20] As opposed to commonly used piezoelectric materials such as quartz or lithium niobate ($LiNbO_3$), several members of the langasite family do not show any phase transition until their melting point around 1500 °C. This high-temperature stability as well as the good piezoelectric properties led to a high scientific and practical interest in these materials being ideal for high-temperature and high-sensitivity applications such as surface acoustic wave (SAW) or bulk acoustic wave (BAW) sensors.[19−23]

Up to now, a large variety of substitution variants has been synthesized in the family of langasites, for example, with compounds exhibiting a wide homogeneity region like AO−TeO_3−Ga_2O_3−XO_2 (A = Pb, Ba, Sr; X = Si, Ge) and PbO−TeO_3−MO−GeO_2 (M = Zn, Co) in the $Ca_3Ga_2Ge_4O_{14}$ structure type.[24] To the best of our knowledge, $Sr_{3-x/2}B_{2-x}Ge_{4+x}O_{14}$ (x = 0.32) is the first boron-containing compound in the $Ca_3Ga_2Ge_4O_{14}$ structure type. Therewith, the important family of langasites can be extended to new noncentrosymmetric substitution variants including boron, which might lead to better piezoelectric properties of potential materials in the future.

Received: May 28, 2014
Published: August 27, 2014

   dx.doi.org/10.1021/ic5012296 | Inorg. Chem. 2014, 53, 9722−9728

EXPERIMENTAL SECTION

Synthesis of $Sr_{3-x/2}B_{2-x}Ge_{4+x}O_{14}$ (x = 0.32). The strontium borogermanate $Sr_{3-x/2}B_{2-x}Ge_{4+x}O_{14}$ (x = 0.32) was synthesized by a nonstoichiometric mixture of precalcined SrO (166 mg; $SrCO_3$ 99+%, Merck, Darmstadt, Germany), GeO_2 (268 mg; 99.99%, ChemPUR, Karlsruhe, Germany), and H_3BO_3 (119 mg; 99.5%, Merck, Darmstadt, Germany) in a NaF−KF (>99%, Fluka/Sigma-Aldrich, St. Louis, MO, USA) flux with a NaF/KF ratio of 0.66:1 (5 mg/11 mg). The reaction mixture and the flux compounds were finely ground in an agate mortar and filled into a platinum crucible (No. 21, FKS Pt/Au, Ögussa, Wien, Austria). The crucible with the sample was positioned in a muffle furnace (HTC 03/16, Nabertherm, Lilienthal, Germany), heated to 1100 °C for 38 h, and then cooled to 400 °C with a cooling rate of 0.05 °C/min before the furnace was switched off. The new compound $Sr_{3-x/2}B_{2-x}Ge_{4+x}O_{14}$ (x = 0.32) crystallized in small, colorless crystals, which were used for the single-crystal X-ray diffraction analysis.

Elementary Analysis. The electron microprobe analyses (EPMA) of strontium and germanium were carried out with a JEOL superprobe 8100 with EDX. The results revealed that the individual Sr/Ge molar ratios of different crystals varied between 1:1.3 and 1:1.7, which means that the compound $Sr_{3-x/2}B_{2-x}Ge_{4+x}O_{14}$ exhibits a phase width ranging from x = 0.1 to 0.6. The mean value of these EDX elemental analyses amounts to a Sr/Ge molar ratio of 1:1.5, which is in good agreement with the determination of the composition from the single-crystal X-ray diffraction data showing a value of Sr/Ge = 1:1.52. As boron and oxygen are not detectable in a reasonable way using this method, their content was determined on the basis of the refinement of the single crystal data (*vide infra*) in combination with the ratio of Sr/Ge.

X-ray Powder Diffraction. The powder X-ray diffraction pattern was obtained in transmission geometry from a flat sample of the product. The measurements were carried out using a STOE STADI P powder diffractometer with Mo Kα1 radiation (Ge monochromator λ = 70.93 pm) in the 2θ range of 2−63° with a step size of 0.15°. Figure S1 of the Supporting Information shows the experimental powder pattern matching the theoretical pattern simulated from single-crystal data. The Rietveld analysis of the powder pattern using the program Topas[25] exhibited a second phase—$SrGe_4O_9$—which adds up to a content of ∼8% of the probed powder (Supporting Information Figure S2 and Table S1).

Single-Crystal Structure Determination. The single-crystal data were collected at room temperature using a Nonius Kappa-CCD diffractometer with a graphite-monochromatized Mo Kα radiation (λ = 71.073 pm). A semi-empirical absorption correction based on equivalent and redundant intensities (Scalepack)[26] was applied to the intensity data. The structure solution and parameter refinement (full-matrix-least-squares against F^2) were performed by using the SHELX-97 software suite with anisotropic atomic displacement parameters for all atoms.[27,28] The structure determination of $Sr_{3-x/2}B_{2-x}Ge_{4+x}O_{14}$ (x = 0.32) revealed that it crystallizes in the trigonal space group $P321$. The Flack parameter of 0.07(2), the GOF of 1.099 as well as the value of $R1$ = 0.0281 for 931 unique reflections with $I \geq 2\sigma(I)$ reflect the correctness of the absolute structure. To ensure that no symmetry operations are missing, the final solution was checked with PLATON.[29] All relevant details of the crystallographic data are summarized in Table 1, the positional parameters are listed in Table 2, and the important bond lengths are listed in Table 3. The program "Diamond" was used for the graphical representation (Figures 1−5) of the structure.[30] Additional crystallographic information is available in the Supporting Information.

Vibrational Spectroscopy. The transmission IR spectra were measured in the spectral range of 4000−550 cm^{-1} with a Bruker Vertex 70 FT-IR spectrometer equipped with a MCT-detector and a focal plane array (FPA) detector (4096 pixel) using a BaF_2 specimen carrier. The single-crystal Raman spectrum of $Sr_{3-x/2}B_{2-x}Ge_{4+x}O_{14}$ (x = 0.32) was measured in the spectral range of 4000−50 cm^{-1} with a HORIBA Jobin Yvon LabRam-HR 800 microspectrometer. The sample was excited using the 532 nm emission line of a frequency-doubled 500 mW Nd:YAG laser under an Olympus 100 × objective lens. The size of the laser spot on the surface was approximately 1 μm.

Table 1. Crystal Data and Structure Refinement of $Sr_{3-x/2}B_{2-x}Ge_{4+x}O_{14}$ (x = 0.32)

empirical formula	$Sr_{3-x/2}B_{2-x}Ge_{4+x}O_{14}$ (x = 0.32)
molar mass, g·mol^{-1}	804.59
crystal system	trigonal
space group	$P321$
powder diffractometer	Stoe Stadi P
radiation	Mo Kα1 (λ = 71.073 pm)
powder data	
a, pm	799.83(2)[a]
c, pm	488.25(2)[a]
V (Å^3)	270.50(2)[a]
single crystal data	
single crystal diffractometer	Enraf-Nonius Kappa CCD
radiation	Mo Kα (λ = 71.073 pm) (graded multilayer X-ray)
a, pm	800.7(2)[a]
c, pm	488.8(2)[a]
V (Å^3)	271.39(8)[a]
formula units per cell	Z = 1
calculated density, g·cm^{-3}	4.923
crystal size, mm^3	0.05 × 0.02 × 0.01
temperature	293(2)[a]
absorption coefficient, mm^{-1}	25.73
F(000)	367
θ range, deg	2.9−37.5
range in hkl	$-13 \leq h \leq 13$, $-13 \leq k \leq 13$, $-8 \leq l \leq 8$
total no. of reflections	5291
independent reflections	961 (R_{int} = 0.0921)
reflections with $I \geq 2\sigma(I)$	931 (R_σ = 0.0443)
data/parameters	961/39
absorption correction	multiscan (Scalepack)[26]
goodness-of-fit on F^2	1.099
flack parameter	0.07(2)[a]
final R indices [$I \geq 2\sigma(I)$]	$R1$ = 0.0270
	$wR2$ = 0.0666
final R indices (all data)	$R1$ = 0.0281
	$wR2$ = 0.0671
largest diff. peak and hole, e·Å^3	1.19/−1.22

[a]Standard deviations in parentheses.

The scattered light was dispersed by an optical grating with 1800 lines mm^{-1} and collected by a 1024 × 256 open electrode CCD detector. No background correction was necessary and the Raman bands were fitted by the built-in spectrometer software LabSpec to second order polynomial and convoluted Gaussian−Lorentzian functions.[31]

RESULTS AND DISCUSSION

Mao et al. just recently succeeded in synthesizing the first two strontium borogermanates, namely, $SrGe_2B_2O_8$ and $Sr_3Ge_2B_6O_{16}$, which were synthesized using the corresponding molar ratios at 900 °C without the use of any flux material.[1] The new compound $Sr_{3-x/2}B_{2-x}Ge_{4+x}O_{14}$ (x = 0.32) crystallizes in the trigonal, noncentrosymmetric space group $P321$ being isotypic to $Ca_3Ga_2Ge_4O_{14}$ and $Sr_3Ga_2Ge_4O_{14}$.[17] The asymmetric unit of $Sr_{3-x/2}B_{2-x}Ge_{4+x}O_{14}$ (x = 0.32) contains two different Ge atoms (Ge1 on the special position 3f and Ge2 on the special position 1a), one Sr atom (3e), three O atoms (O1 and O2 at 6g, O3 at 2d) and one B^{3+}/Ge^{4+} mixed site at 2d. The Ge1 atoms at the special site 3f are coordinated tetrahedrally by four oxygen atoms whereas the Ge2 atoms at the special site 1a are coordinated octahedrally by six oxygen

dx.doi.org/10.1021/ic5012296 | Inorg. Chem. 2014, 53, 9722−9728

Table 2. Atomic Coordinates, Site Occupancy Factor (s.o.f.) and Equivalent Isotropic Displacement Parameters U_{eq} of $Sr_{3-x/2}B_{2-x}Ge_{4+x}O_{14}$ (x = 0.32) with Standard Deviations in Parentheses

atom	Wyckoff position	x/a	y/b	z/c	U_{eq}[a] (Å^2)	s.o.f.
Sr1	3*e*	0.43266(6)	0	0	0.01073(2)	0.95
Ge1	3*f*	0	0.738 77(6)	0.5	0.00886(2)	1
Ge2	1*a*	0	0	0	0.00699(2)	1
Ge3	2*d*	2/3	1/3	0.4844(5)	0.0089(6)	0.16
B1	2*d*	2/3	1/3	0.4844(5)	0.0089(6)	0.84
O1	6*g*	0.8224(4)	0.5242(4)	0.3443(5)	0.0135(4)	1
O2	6*g*	0.1162(4)	0.8976(4)	0.2282(5)	0.0109(4)	1
O3	2*d*	2/3	1/3	0.7713(1)	0.0159(8)	1

[a] U_{eq} is defined as one third of the trace of the orthogonalized U_{ij} tensor.

Table 3. Interatomic Distances (pm) in $Sr_{3-x/2}B_{2-x}Ge_{4+x}O_{14}$ (x = 0.32)

the 3*e* dodecahedron[a]			the 1*a* octahedron[a]		
Sr1−O2	250.2(2)	(2 ×)	Ge2−O2	188.3(2)	(6 ×)
Sr1−O1′	253.6(3)	(2 ×)			
Sr1−O3	262.4(2)	(2 ×)			
Sr1−O1′′	279.8(3)	(2 ×)	the 2*d* tetrahedron		
			B1/Ge3−O1	156.7(3)	(3 ×)
			B1/Ge3−O3	140.2(6)	(1 ×)
O1−O1	244.6(1)	(2 ×)			
O1−O1′	417.3(5)	(1 ×)	the 3*f* tetrahedron		
O1−O2	311.5(3)	(2 ×)	Ge1−O1	176.3(2)	(2 ×)
O1−O2′	336.4(8)	(2 ×)	Ge1−O2	175.0(2)	(2 ×)
O1−O3	313.5(1)	(4 ×)			
O1−O3′	370.6(4)	(2 ×)			
O1−O3″	463.7(4)	(2 ×)			
O2−O2	264.8(4)	(1 ×)			
O2−O3	311.2(3)	(2 ×)			

[a] Standard deviations in parentheses.

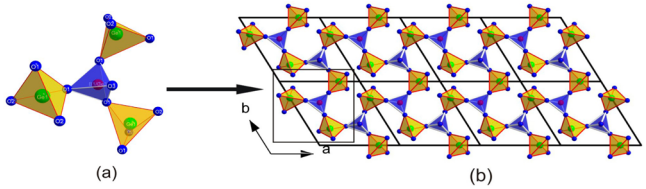

Figure 1. B^{3+}/Ge^{4+} tetrahedra (blue) connected with GeO_4 tetrahedra (beige) (a) form a layer of tetrahedra parallel to the *ab* plane (b).

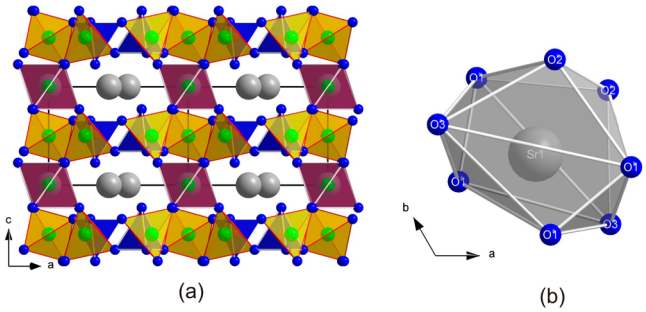

Figure 2. (a) Structure of $Sr_{3-x/2}B_{2-x}Ge_{4+x}O_{14}$ (x = 0.32). Layers of GeO_4 and $B^{3+}/Ge^{4+}O_4$ tetrahedra or a three-dimensional B−Ge−O network interconnected via GeO_6 octahedra (purple). (b) SrO_8 polyhedron.

atoms. At this point it should be mentioned that in $Ca_3Ga_2Ge_4O_{14}$ and $Sr_3Ga_2Ge_4O_{14}$, the octahedrally coordinated sites 1*a* are mixed occupied with Ga^{3+} and Ge^{4+} cations. In

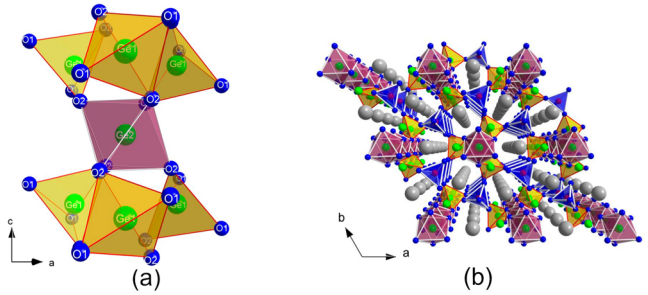

Figure 3. (a) Voronkov block consisting of an GeO_6 octahedron and six GeO_4 tetrahedra; (b) Crystal structure of $Sr_{3-x/2}B_{2-x}Ge_{4+x}O_{14}$ (x = 0.32) down [001] exhibiting the channels created through the GeO_4−B/GeO_4 network and occupied by Sr atoms (gray).

$Sr_{3-x/2}B_{2-x}Ge_{4+x}O_{14}$ (x = 0.32), the special site 1*a* is completely occupied with Ge^{4+} cations (Ge2). The mixed position at 2*d* (B^{3+}/Ge^{4+}) is coordinated tetrahedrally by four oxygen atoms. The structure determination revealed that the latter position is statistically occupied by B^{3+} (84%) and Ge^{4+} (16%). The Sr^{2+} is coordinated by eight oxygen atoms in form of a distorted Thomson cube. This position exhibits a slight deficiency which amounts to ∼5%.

The B/GeO_4 tetrahedra possess one terminal oxygen atom (O3) and three bridging corners (O1) to GeO_4 tetrahedra (Figure 1a). The bond lengths B/Ge−O have values of 156.7(3) pm to the oxygen atoms shared with the GeO_4 tetrahedra and 140.4(6) pm to the terminal oxygen atom (O3) with an average bond length of 152.6 pm. This

dx.doi.org/10.1021/ic5012296 | Inorg. Chem. 2014, 53, 9722−9728

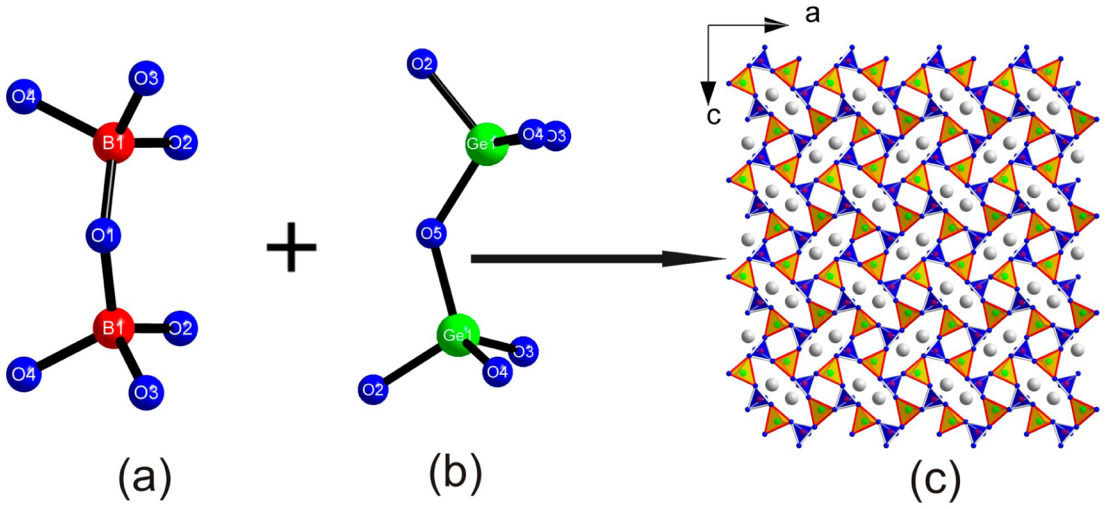

Figure 4. (a) B_2O_7 unit, (b) Ge_2O_7 unit, (c) view of the structure of $SrGe_2B_2O_8$ down the *b* axis.[1]

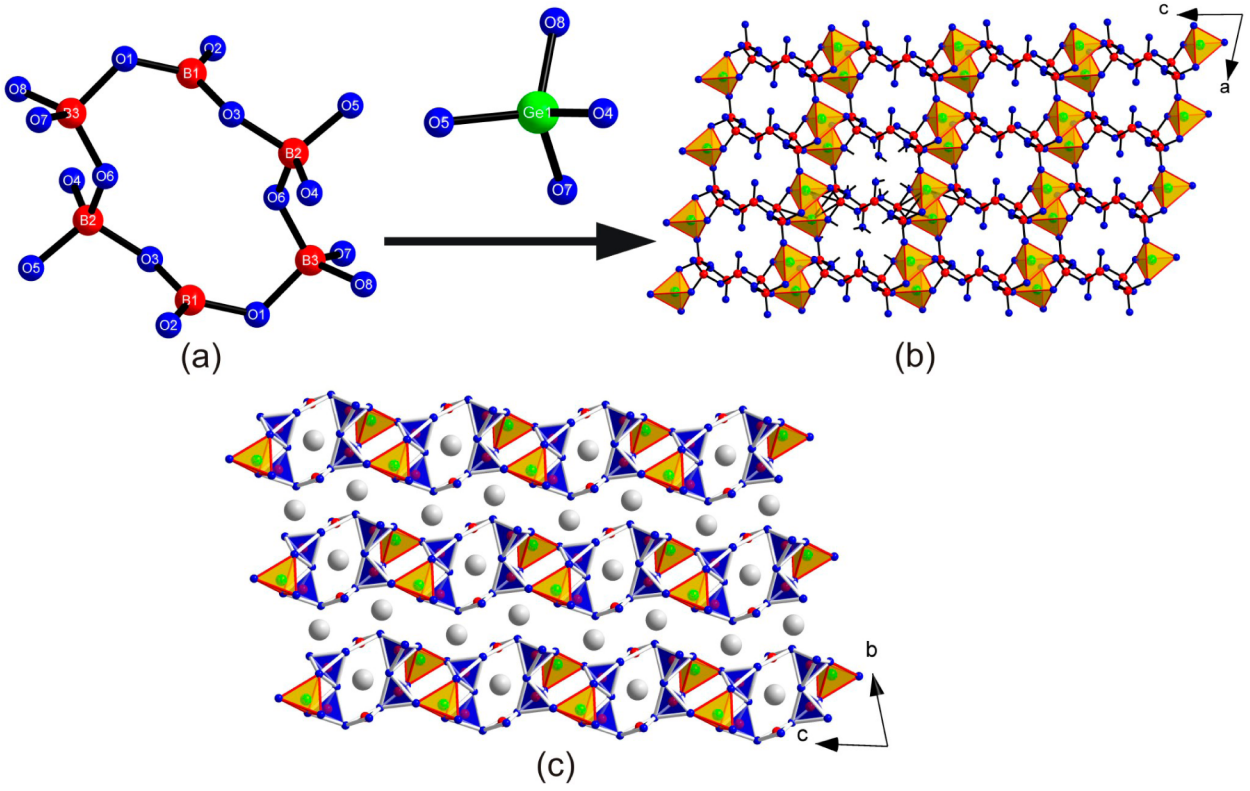

Figure 5. (a) B_6O_{16} cluster unit, (b) two-dimensional $[Ge_2B_6O_{16}]^{6-}$ layer in the *ac* plane, and (c) view of the structure of $Sr_3Ge_2B_6O_{16}$ along the *a* axis.[1]

divergence in the mean B/Ge−O distance from our compound compared to the known average value of 147.6 pm[32] in BO_4 tetrahedra is interpreted due to a mixed occupation B^{3+}/Ge^{4+}, because the Ge−O distance is longer due to the larger ionic radius of germanium. The O−B/Ge−O bond angles within this tetrahedron range from 102.3(2) to 115.9(2)°. The Ge−O bond lengths within the GeO_4 tetrahedra (175.0(2)−176.3(3) pm) are significantly shorter than those of the GeO_6 octahedra (188.3(2) pm). The O−Ge−O angels of the tetrahedra range from 104.8(2)−125.2(2)° depending on the connected units, and the bond angels within the octahedra range from 88.5(1) to 93.8(2)°. The Ge(1)O_4 tetrahedra share two corners (O1) with the B/GeO_4 tetrahedra and two oxygen atoms (O2) with GeO_6 units. The GeO_6 octahedra are connected via six oxygen atoms (O2) to six GeO_4 tetrahedra. The Sr−O bond length within the SrO_8 polyhedron vary in the range of 250.2(3)−279.8(3) pm. The edge lengths of the SrO_8 polyhedron vary in the range of 244.6(1)−463.7(4) pm whereas the shortest edge O1−O1 is shared with the B^{3+}/Ge^{4+} tetrahedron and the longest edge O1−O3″, parallel to [100], forms the diagonal of the polyhedrons base. For information about all the edge lengths of the polyhedron see Table 3. The SrO_8 polyhedron consist of 8 vertices and 12 faces with trigonal shape and can be considered as a distorted trigonal dodecahedron as the same

dx.doi.org/10.1021/ic5012296 | *Inorg. Chem.* 2014, 53, 9722−9728

polyhedron can also be observed in the isotypic phases $Ca_3Ga_2Ge_4O_{14}$ and $Sr_3Ga_2Ge_4O_{14}$.[22] The faces forming the base are slightly folded along the diagonal O1−O3″ and therefore the angle between the faces is 177.5(3)°. This means that a small change of the *z* coordinate of the oxygen atom would transfer the dodecahedron into a decahedron (10 faces). This transformation can be observed e.g. in the structure of $Ca_3TaGa_3Si_2O_{14}$.[33] The strontium cation in the center of the polyhedron is displaced along the *a* axis from the short O2−O2 edge shared with the germanium octahedron (position 1*a*) toward the longer O1−O1 edge (Figure 2b). The observed bond angels and lengths within the structure are in good agreement to those of other borogermanates and the isotypic phase $Sr_3Ga_2Ge_4O_{14}$.[1,2,4,17,22,23]

The connection of these units leads to a very interesting framework which can be separated in two different planes. The GeO_4 and B/GeO_4 units form a layer of tetrahedra which are arranged parallel to the *ab* plane. This unique connection of B/GeO_4 tetrahedra with GeO_4 tetrahedra forms rings built up of 12 tetrahedra (Figure 1b). The GeO_6 octahedra, whose center atom (Ge2) is offset in the direction of the crystallographic *c* axis, bridge the $Ge(1)O_4$ tetrahedra of the above-described layer to the $Ge(1)O_4$ tetrahedra of the next layer (Figure 2a). This arrangement of an octahedron (GeO_6) sharing vertices with six tetrahedra (GeO_4) forms so-called Voronkov blocks (Figure 3a).[34] The tetrahedra of these Voronkov blocks are linked through the B/GeO_4 tetrahedra (position 2*d*) and form a characteristic framework. This framework can also be found in various other structures of phosphates, germanates, gallates, and silicates.[35,36]

Alternatively, the structure can be described starting with the connection of the GeO_6 octahedra via corner sharing to the $Ge(1)O_4$ tetrahedra leading to the formation of $1D[Ge_4O_{12}]$ chains along the *c* axis. Each chain is connected with six other chains via six B/GeO_4 tetrahedra. This arrangement of polyhedra forms channels along the *c* axis in which the 8-fold coordinated Sr^{2+} cations are located (Figure 3b). The Sr^{2+} cations are positioned in the same *ab* plane as the octahedrally coordinated Ge(2) atoms (Figure 2a).

As mentioned earlier, the phase $Sr_{3-x/2}B_{2-x}Ge_{4+x}O_{14}$ (x = 0.32) is isotypic to $Ca_3Ga_2Ge_4O_{14}$ and $Sr_3Ga_2Ge_4O_{14}$,[17] however these phases exhibit slightly larger lattice parameters due to the larger ionic radius of gallium compared to boron. The replacement of Ca^{2+} ions by larger Sr^{2+} ions in the structure of $Ca_3Ga_2Ge_4O_{14}$ leads to an anisotropic increase of the lattice parameters. The *a* axis increases from 806.9 to 827.7(2) pm and the *c* axis from 496.7 to 504.2(1) pm in $Sr_3Ga_2Ge_4O_{14}$.[22,23] Within the here presented compound $Sr_{3-x/2}B_{2-x}Ge_{4+x}O_{14}$ (x = 0.32), both the *a* axis (800.7(1) pm) and the *c* axis (488.8(1) pm) are slightly shorter than in those above-mentioned. This contraction is due to the smaller ionic radius of boron compared to gallium. These two phases also possess positions with mixed occupations, but in comparison to $Sr_{3-x/2}B_{2-x}Ge_{4+x}O_{14}$ (x = 0.32), different crystallographic positions exhibit the mixed occupation. Within our structure, the B^{3+}/Ge^{4+} mixed site is located at 2*d*, the positions 1*a* and 3*f* are fully occupied by Ge^{4+} ions and the position 3*e* is occupied by Sr^{2+} showing a slight deficiency (~5%). In $Ca_3Ga_2Ge_4O_{14}$, the position 2*d* is occupied exclusively by Ge^{4+} ions and at the sites 1*a* and 3*f* both cations Ga^{3+} and Ge^{4+} are located at a ratio of 0.4:0.6 and 0.53:0.47, respectively. Within $Sr_3Ga_2Ge_4O_{14}$, the positions 1*a* and 3*f* are occupied by Ga^{3+} and Ge^{4+} ions and the site 2*d* is exclusively filled with Ge^{4+} ions. Various other isotypic phases of the langasite family also show disorders in the 1*a*, 3*f*, and 2*d* positions and vacancies in the 3*e* position.[20,22,24] Maksimov et al. already observed that the smaller ions occupy the 2*d* position and form small-sized tetrahedra, whereas larger ions form large-sized tetrahedra in the 3*f* position in various other members of the Langasite family crystallizing in the $Ca_3Ga_2Ge_4O_{14}$ structure type.[37] From this observation it is reasonable that the B^{3+} cations in $Sr_{3-x/2}B_{2-x}Ge_{4+x}O_{14}$ (x = 0.32) locate at the site 2*d*.

The comparison of the SrO_8 dodecahedron of $Sr_3Ga_2Ge_4O_{14}$ with the SrO_8 dodecahedron of $Sr_{3-x/2}B_{2-x}Ge_{4+x}O_{14}$ (x = 0.32) reveals various interesting differences. The average Sr−O bond length with a value of 264.8 pm in $Sr_3Ga_2Ge_4O_{14}$ is slightly larger than in $Sr_{3-x/2}B_{2-x}Ge_{4+x}O_{14}$ with a value of 261.5 pm. Within $Sr_{3-x/2}B_{2-x}Ge_{4+x}O_{14}$ (x = 0.32), the shortest edge of the SrO_8 polyhedron is shared with the mixed occupied B/Ge tetrahedron (position 3*e*). In contrary, the shortest edge of the SrO_8 polyhedron in $Sr_3Ga_2Ge_4O_{14}$ is shared with the mixed Ga/Ge position. The longest edge within the polyhedra of both phases however is the diagonal of the base. Furthermore, it is interesting to note that the shortest edge length within $Sr_{3-x/2}B_{2-x}Ge_{4+x}O_{14}$ (x = 0.32) with a value of 244.6(1) pm is slightly shorter than in $Sr_3Ga_2Ge_4O_{14}$ (263.4(1) pm). On the other side, the longest edge within the dodecahedron of $Sr_{3-x/2}B_{2-x}Ge_{4+x}O_{14}$ (x = 0.32) is increasing to a value of 463.7(4) pm in comparison with 415.7(2) pm in the dodecahedron of $Sr_3Ga_2Ge_4O_{14}$. These differences in the length can be interpreted as a result of the formal substitution of gallium through boron (boron occupies the Ge site 2d and Ge occupies the original mixed Ga/Ge sites).[23] As the size of the dodecahedron around the special site 3*e* is crucial for the piezoelectric properties, this expansion of the structure of $Sr_{3-x/2}B_{2-x}Ge_{4+x}O_{14}$ (x = 0.32) along [100] compared to $Sr_3Ga_2Ge_4O_{14}$ could cause better piezoelectric properties.[22,36,38]

Furthermore, it is worthwhile to compare the structure of $Sr_{3-x/2}B_{2-x}Ge_{4+x}O_{14}$ (x = 0.32) with other strontium borogermanates and alkaline-earth borogermanates in general. Similar $1D[Ge_4O_{12}]$ chains can be found within $Cd_{12}Ge_{17}B_8O_{58}$[2] which crystallizes in the space group $P\bar{4}$. But in comparison to $Sr_{3-x/2}B_{2-x}Ge_{4+x}O_{14}$ (x = 0.32), the BO_4 tetrahedra within $Cd_{12}Ge_{17}B_8O_{58}$ form a B_2O_7 dimer via vertex sharing. Four of those B_2O_7 dimers are connected via one central GeO_4 tetrahedron which leads in summary to a different anionic network. So far, there are only two other strontium borogermanates known: $SrGe_2B_2O_8$ crystallizing in the orthorhombic space group *Pnma* (No. 62) and $Sr_3Ge_2B_6O_{16}$ in the centrosymmetric space group $P\bar{1}$ (No. 2). Within $SrGe_2B_2O_8$, the Ge and B atoms are coordinated tetrahedrally. The BO_4 tetrahedra share three corners with the GeO_4 tetrahedra and one corner with a second BO_4 tetrahedron and *vice versa*. The connection of the tetrahedra leads to Ge_2O_7 and B_2O_7 units which form a three-dimensional $[Ge_2B_2O_8]^{2-}$ network. This network exhibits channels along the *b* axis in which the eight-coordinated Sr^{2+} cations are positioned (Figure 4).[1] $Sr_3Ge_2B_6O_{16}$ is isostructural with $Ba_3Ge_2B_6O_{16}$ and consist of GeO_4 tetrahedra, BO_4 tetrahedra, BO_3 groups, and eight-coordinated Sr^{2+}. The structure is built up of layers of BO_4 and BO_3 units parallel to the *ac* plane (Figure 5). The layers are bridged by corner-sharing GeO_4 tetrahedra similar to the GeO_6 octahedra which bridge the layers in $Sr_{3-x/2}B_{2-x}Ge_{4+x}O_{14}$ (x = 0.32). The Sr^{2+} cations are eight-coordinated by oxygen atoms and positioned in tunnels along the *a* axis formed by the B_6O_{16} clusters.[1] In comparison to the just mentioned compounds,

dx.doi.org/10.1021/ic5012296 | Inorg. Chem. 2014, 53, 9722−9728

$Ca_{10}Ge_{16}B_6O_{51}$ is also rather germanium rich than boron rich just as $Sr_{3-x/2}B_{2-x}Ge_{4+x}O_{14}$ (x = 0.32). Its structure features corner-sharing GeO_4 tetrahedra and GeO_6 octahedra which lead to $[Ge_4O_{10.75}]_n$ layers. These layers are bridged by BO_4 tetrahedra and B_2O_7 dimers. The three-dimensional network forms different tunnels which are occupied by Ca^{2+} cations.[2]

In summary, the structure analysis and comparison shows that the various structural units within $Sr_{3-x/2}B_{2-x}Ge_{4+x}O_{14}$ (x = 0.32) can also be found in other borogermanates but the connection of the units leads to a unique network which is isotypic to $Ca_3Ga_2Ge_4O_{14}$ and $Sr_3Ga_2Ge_4O_{14}$. To the best of our knowledge, it is the first borogermanate with a mixed tetrahedral B^{3+}/Ge^{4+} position as well as the first boron containing compound in the $Ca_3Ga_2Ge_4O_{14}$ structure. As the structure of $Sr_{3-x/2}B_{2-x}Ge_{4+x}O_{14}$ (x = 0.32) is quite different from those of $SrGe_2B_2O_8$ and $Sr_3Ge_2B_6O_{16}$, it depicts that slightly different molar ratios of the educts and the use of a flux material can lead to the formation of essential different structures.

The IR and Raman spectra of $Sr_{3-x/2}B_{2-x}Ge_{4+x}O_{14}$ (x = 0.32) are displayed in Figures 6 and 7, respectively. The IR spectrum

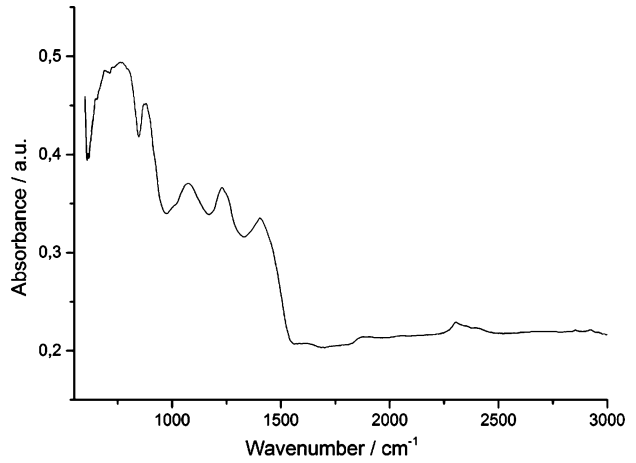

Figure 6. Absorbance IR spectrum of $Sr_{3-x/2}B_{2-x}Ge_{4+x}O_{14}$ (x = 0.32) in the range of 500−3000 cm^{-1}.

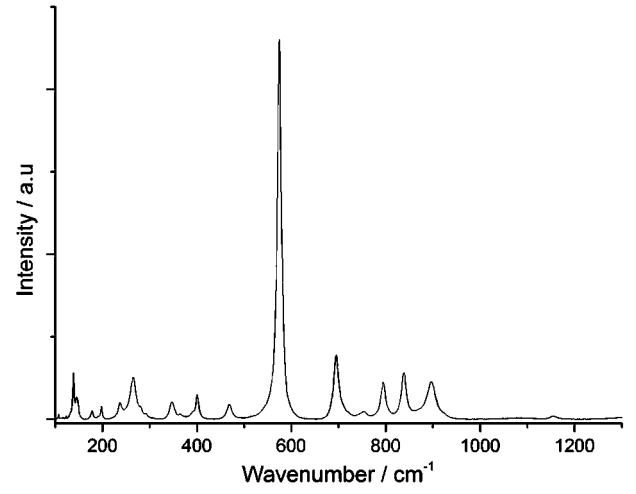

Figure 7. Raman spectrum of $Sr_{3-x/2}B_{2-x}Ge_{4+x}O_{14}$ (x = 0.32) in the range of 50−1300 cm^{-1}.

shows a series of different absorption bands with frequencies below 1500 cm^{-1}, which can be associated with various vibrations of the different units within the crystal. The intense absorption bands between 690 and 860 cm^{-1} can be related to various modes within the different GeO_4 tetrahedra and GeO_6 octahedra as well as to vibrational modes of the BO_4 tetrahedra.[39−42] In this range, various bands are intermixed and therefore it is impossible to distinguish all individual bands. The peak at 870 cm^{-1} is typical for the asymmetric stretching mode of Ge−O−Ge bridges between the GeO_4 tetrahedra and the GeO_6 octahedra.[39,43] The detached peak at 1070 cm^{-1} is associated with an asymmetric stretching mode of the BO_4 tetrahedra.[43,44] In general, there are several absorption bands between 800 and 1100 cm^{-1} which are due to stretching modes within the BO_4 tetrahedra.[45,46] Terkadeo et al. assume that the peak at 1400 cm^{-1} might be a combinational tone of two vibration modes of Ge−O−Ge bonds.[47]

Furthermore, we used Raman spectroscopy to render the new phase $Sr_{3-x/2}B_{2-x}Ge_{4+x}O_{14}$ (x = 0.32) more precisely. The Raman spectrum (Figure 7) displays a series of peaks which can be related to the different structural units. The peaks with lower frequencies than ∼300 cm^{-1} are assigned to various translation and rotational modes of the structural units.[48,49] The bands in the range of 400 to 500 cm^{-1} can probably be assigned to the bending modes within the GeO_4 tetrahedra and those in the range of 700 to 850 cm^{-1} may come from the symmetric and asymmetric stretching modes of the GeO_4 tetrahedra.[49,50] For example, Origlieri et al. ascribe the peak at 400 cm^{-1} to a Ge−O−Ge bending vibration within the GeO groups in the germanate $PbFeGe_3O_7(OH)_2{\cdot}H_2O$.[48] Peaks in the range of 300 to 450 cm^{-1} can be assigned to the bending of the BO_4 tetrahedra, the peak at 570 cm^{-1} to the BO_4 symmetric stretching vibration, the peak at 840 cm^{-1} to the BO_4 asymmetric stretching vibration, and the small peak at 1160 cm^{-1} can be assigned to the distortion of the BO_4 tetrahedra.[51−53]

CONCLUSIONS

In summary, we were successful in synthesizing a new strontium borogermanate with the composition $Sr_{3-x/2}B_{2-x}Ge_{4+x}O_{14}$ (x = 0.32) being the first boron containing member of the langasite family. The EDX elemental analyses depicted that the compound shows a phase width with a varying ratio of Sr/Ge. The structure determination revealed that it crystallizes in a noncentrosymmetric space group ($P321$) being isotypic to $Ca_3Ga_2Ge_4O_{14}$ and $Sr_3Ga_2Ge_4O_{14}$. Formally, GeO_4 and BO_4 tetrahedra form layers perpendicular to the c axis, which are interconnected through GeO_6 octahedra. This arrangement of structural units forms channels in which the 8-fold coordinated Sr^{2+} cations are positioned. As several compounds of the langasite family are already promising piezoelectric materials, the herein reported new boron containing phase $Sr_{3-x/2}B_{2-x}Ge_{4+x}O_{14}$ (x = 0.32) leads to a wider range of compositions which could exhibit further interesting physical properties as the properties change distinctly from compound to compound.

ASSOCIATED CONTENT

Supporting Information

X-ray crystallographic files in CIF format, simulated and measured X-ray diffraction patterns, and Rietveld refinement plots of the XRD powder pattern. This material is available free of charge via the Internet at http://pubs.acs.org. Additional details of the crystal structure investigations may be obtained from Fachinformationszentrum Karlsruhe, 76344 Eggenstein-

dx.doi.org/10.1021/ic5012296 | Inorg. Chem. 2014, 53, 9722−9728

Leopoldshafen, Germany (fax: +49−7247−808−666; e-mail: crysdata@fiz-karlsruhe.de, http://www.fiz-informationsdienste.de/en/DB/icsd/depotanforderung.html) on quoting the deposition number CSD-427780.

AUTHOR INFORMATION

Corresponding Author

*E-mail: Hubert.Huppertz@uibk.ac.at. Fax: +43 (512) 507-57099.

Notes

The authors declare no competing financial interest.

ACKNOWLEDGMENTS

Special thanks goes to G. Sohr, Dept. of Chemistry, Univ. of Innsbruck, for the support with the IR spectroscopy, Univ. assistant Dr. R. Tappert, Institute of Mineralogy and Petrography, Univ. of Innsbruck for the support with the Raman spectroscopy, and Univ. Prof. Dr. R. Stalder, Institute of Mineralogy and Petrography, Univ. of Innsbruck for the access to the IR microscope and the Raman spectrometer. We are also grateful to Mrs. M. Tribus, Institute of Mineralogy and Petrography, Univ. of Innsbruck, for her help with the EDX measurements.

REFERENCES

(1) Hao, Y. C.; Hu, C. L.; Xu, X.; Kong, F.; Mao, J. G. *Inorg. Chem.* **2013**, *52*, 13644−13650.
(2) Xu, X.; Hu, C. L.; Kong, F.; Zhang, J. H.; Mao, J. G. *Inorg. Chem.* **2011**, *50*, 8861−8868.
(3) Zhang, J. H.; Hu, C. L.; Xu, X.; Kong, F.; Mao, J. G. *Inorg. Chem.* **2011**, *50*, 1973−1982.
(4) Zhang, J. H.; Kong, F.; Mao, J. G. *Inorg. Chem.* **2011**, *50*, 3037−3043.
(5) Zhang, J.-H.; Kong, F.; Xu, X.; Mao, J.-G. *J. Solid State Chem.* **2012**, *195*, 63−72.
(6) Callister, W. D.; Rethwisch, D. G. *Materialwissenschaften und Werkstofftechnik;* Wiley-VCH: Weinheim, Germany, 2013.
(7) Nikogosyan, D. *Nonlinear Optical Crystals: A Complete Survey: A Complete Survey;* Springer: New York, 2006.
(8) Huang, Y.-Z.; Wu, L.-M.; Wu, X.-T.; Li, L.-H.; Chen, L.; Zhang, Y.-F. *J. Am. Chem. Soc.* **2010**, *132*, 12788−12789.
(9) Chi, E. O.; Ok, K. M.; Porter, Y.; Halasyamani, P. S. *Chem. Mater.* **2006**, *18*, 2070−2074.
(10) Zhao, W.; Pan, S.; Wang, Y.; Yang, Z.; Wang, X.; Han, J. *J. Solid State Chem.* **2012**, *195*, 73−78.
(11) Goodey, J.; Broussard, J.; Halasyamani, P. S. *Chem. Mater.* **2002**, *14*, 3174−3180.
(12) Zhang, H.-X.; Zhang, J.; Zheng, S.-T.; Wang, G.-M.; Yang, G.-Y. *Inorg. Chem.* **2004**, *43*, 6148−6150.
(13) Kong, F.; Jiang, H.-L.; Hu, T.; Mao, J.-G. *Inorg. Chem.* **2008**, *47*, 10611−10617.
(14) Xiong, D. B.; Zhao, J. T.; Chen, H. H.; Yang, X. X. *Chem.—Eur. J.* **2007**, *13*, 9862−9865.
(15) Belokoneva, E. L.; Simonov, M. A.; Butashin, A. V.; Mill, B. V.; Belov, N. V. *Dokl. Akad. Nauk SSSR* **1980**, *255*, 1099.
(16) Belokoneva, E.; Belov, N. *Dokl. Akad. Nauk SSSR* **1981**, *260*, 1363−1366.
(17) Kaminskii, A.; Belokoneva, E.; Mill, B.; Pisarevskii, Y. V.; Sarkisov, S.; Silvestrova, I.; Butashin, A.; Khodzhabagyan, G. *Phys. Status Solidi A* **1984**, *86*, 345−362.
(18) Mill, B.; Belokoneva, E.; Fukuda, T. *Russ. J. Inorg. Chem.* **1998**, *43*, 1168−1175.
(19) Mill, B.; Maksimov, B.; Pisarevskii, Y. V.; Danilova, N.; Pavlovska, A.; Werner, S.; Schneider, J. *Kristallografiya* **2004**, *49*, 60−69.
(20) Ohsato, H.; Morikoshi, H. *Trans. Electr. Electron. Mater.* **2012**, *13*, 51−59.
(21) Adachi, M.; Kimura, T.; Miyamoto, W.; Chen, Z.; Kawabata, A. *J. Korean Phys. Soc.* **1998**, *32*, 1274−1277.
(22) Mill, B.; Klimenkova, A.; Maximov, B.; Molchanov, V.; Pushcharovsky, D. Y. *Kristallografiya* **2007**, *52*, 785−794.
(23) Dudka, A.; Mill, B. *Kristallografiya* **2012**, *57*, 49−56.
(24) Mill, B. *Russ. J. Inorg. Chem.* **2010**, *55*, 1611−1616.
(25) *TOPAS,* v. 4.2; Bruker AXS: Karlsruhe, Germany, 2009.
(26) Otwinowski, Z.; Minor, W. *Methods Enzymol.* **1997**, *276*, 307−326.
(27) Sheldrick, G. *SHELXL-97: Program for the Refinement of Crystal Structures;* University of Göttingen: Göttingen, Germany, 1997, 2006.
(28) Sheldrick, G. M. *Acta Crystallogr., Sect. A* **2007**, *64*, 112−122.
(29) Spek, A. *J. Appl. Crystallogr.* **1999**, *32*, 837−838.
(30) Impact, C. *DIAMOND—Crystal and Molecular Structure Visualization;* 2005. http://www.crystalimpact.com/diamond.
(31) *LabSpec;* Horiba Jobin Yvon S.A.S.: Villeneuve d'Ascq, France, 2010.
(32) Hawthorne, F. C.; Burns, P. C.; Grice, J. D. *Rev. Mineral. Geochem.* **1996**, *33*, 41−115.
(33) Klimenkova, A.; Maximov, B.; Molchanov, V.; Mill', B.; Rabadanov, M.; Pisarevsky, Y. V.; Pushcharovsky, D. Y. *Kristallografiya* **2007**, *52*, 215−220.
(34) Voronkov, A. A.; Ilyukhin, V. V.; Belov, N. V. *Kristallografiya* **1975**, *20*, 556−566.
(35) Gurbanova, O.; Belokoneva, E. *Kristallografiya* **2006**, *51*, 577−583.
(36) Belokoneva, E.; Stefanovich, S. Y.; Pisarevskii, Y. V.; Mosunov, A. *Russ. J. Inorg. Chem.* **2000**, *45*, 1642−1651.
(37) Maksimov, B.; Molchanov, V.; Mill, B.; Belokoneva, E.; Rabadanov, M. K.; Pugacheva, A.; Pisarevskii, Y. V.; Simonov, V. *Kristallografiya* **2005**, *50*, 751−758.
(38) Ohsato, H. *Trans. Electr. Electron. Mater.* **2012**, *13*, 171−176.
(39) Kamitsos, E.; Yiannopoulos, Y.; Varsamis, C.; Jain, H. *J. Non-Cryst. Solids* **1997**, *222*, 59−68.
(40) Culea, E.; Pop, L.; Bosca, M. *J. Alloys Compd.* **2010**, *505*, 754−757.
(41) Di Martino, D.; Santos, L.; Marques, A.; Almeida, R. *J. Non-Cryst. Solids* **2001**, *293*, 394−401.
(42) Mansour, E.; El-Damrawi, G.; Fetoh, R.; Doweidar, H. *Eur. Phys. J. B* **2011**, *83*, 133−141.
(43) Blaszczak, K.; Adamczyk, A. *J. Mol. Struct.* **2001**, *596*, 61−68.
(44) Reshak, A. H.; Chen, X.; Song, F.; Kityk, I.; Auluck, S. *J. Phys.: Condens. Mater.* **2009**, *21*, 205402.
(45) Hinteregger, E.; Heymann, G.; Hofer, T. S.; Huppertz, H. *Z. Naturforsch.* **2012**, *67*, 605−613.
(46) Ren, M.; Lin, J.; Dong, Y.; Yang, L.; Su, M.; You, L. *Chem. Mater.* **1999**, *11*, 1576−1580.
(47) Terakado, N.; Tanaka, K. *J. Non-Cryst. Solids* **2008**, *354*, 1992−1999.
(48) Origlieri, M. J.; Yang, H.; Downs, R. T.; Posner, E. S.; Domanik, K. J.; Pinch, W. W. *Am. Mineral.* **2012**, *97*, 1812−1815.
(49) Orera, A.; Sanjuán, M.; Kendrick, E.; Orera, V.; Slater, P. *J. Chem. Mater.* **2010**, *20*, 2170−2175.
(50) Rodríguez-Reyna, E.; Fuentes, A. F.; Maczka, M.; Hanuza, J.; Boulahya, K.; Amador, U. *Solid State Sci.* **2006**, *8*, 168−177.
(51) Hu, X.; Wang, J.; Teng, B.; Loong, C.-K.; Grimsditch, M. *J. Appl. Phys.* **2005**, *97*, 033501−033501−033505.
(52) Pascuta, P.; Lungu, R.; Ardelean, I. *J. Mater. Sci.: Mater. Electron.* **2010**, *21*, 548−553.
(53) Grzechnik, A.; Chizmeshya, A.; Wolf, G.; McMillan, P. *J. Phys.: Condens. Mater.* **1998**, *10*, 221.